JOC The Journal of Organic Chemistry

ARTICLE

pubs.acs.org/joc

Characterization and Magnetic Properties of a "Super Stable" Radical 1,3-Diphenyl-7-trifluoromethyl-1,4-dihydro-1,2,4-benzotriazin-4-yl

Christos P. Constantinides,[†] Panayiotis A. Koutentis,*[,‡] Harry Krassos,[‡] Jeremy M. Rawson,[†] and Anastasios J. Tasiopoulos[‡]

[†]Department of Chemistry, The University of Cambridge, Lensfield Road, Cambridge CB2 1EW, United Kingdom

[‡]Department of Chemistry, University of Cyprus, P.O. Box 20537, 1678 Nicosia, Cyprus,

Supporting Information

ABSTRACT: 1,3-Diphenyl-7-trifluoromethyl-1,4-dihydro-1,2,4-benzotriazin-4-yl (**4**), prepared in high yield *via* the catalytic oxidation of the corresponding amidrazone **5** by using Pd/C (1.6 mol %) and 1,8-diazabicyclo[5.4.0]undec-7-ene (0.1 equiv) in air, is stable in dichloromethane solutions in the presence of MnO_2 and $KMnO_4$. Furthermore, radical **4** is thermally stable well past its melting point (160−161 °C) with a decomposition onset temperature of 288 °C. X-ray studies show that radical **4** packs in equidistant slipped π-stacks along the *a* axis. Cyclic voltammetry shows two fully reversible waves, corresponding to the −1/0, 0/+1 processes. EPR studies indicate that the spin density is mainly delocalized on the triazinyl fragment of the heterocycle. Magnetic susceptibility measurements in the 5−300 K region showed that the radical obeys Curie−Weiss behavior down to 10 K (C = 0.376 emu·K·mol^{-1} and θ = +1.41 K) consistent with weak ferromagnetic interactions between S = 1/2 radicals. Subsequent fitting of the magnetic data to a 1D ferromagnetic chain model provided an excellent fit (g = 2.00, J/k = +1.49 K) down to 10 K but failed to reproduce the subsequent decrease in χT at lower temperatures, which has been ascribed to the onset of weaker antiferromagnetic interactions between ferromagnetic chains.

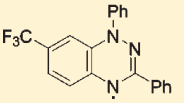

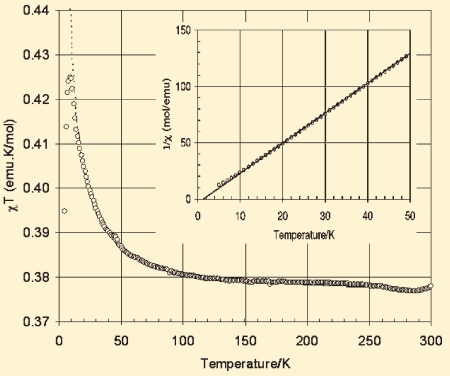

INTRODUCTION

In the past couple of decades we have witnessed remarkable advances in the field of π-electronic materials, specifically in the field of organic molecular magnets as a number of organic radicals have shown magnetic properties previously observed only in metals, their oxides and ceramics.[1] Among all of the major classes of stable or persistent organic/organo-main group radicals the families of nitroxide and nitronyl nitroxide radicals have been particularly well studied as potential magnetic materials.[2] They have exhibited a range of ferromagnetic properties that include one-dimensional (1D) Heisenberg-type linear intrachain,[3] two-dimensional (2D)[4] and bulk ferromagnetism.[5] Other well studied radical families are the heterocyclic thiazyl[6a] and selenazyl radicals[6b−d] and triphenylmethyl[7] and verdazyl radicals.[8] The latter radical family is less studied and stems from the work of delocalized hydrazyl radicals.

Verdazyls are easily prepared[9] and generally air- and moisture-stable where the stability does not require bulky substituents.[10] The first magnetic studies were performed on 1,3,5-triphenylverdazyl in 1973 and showed Heisenberg-type linear chain antiferromagnetic interactions.[11] Small structural changes led to verdazyls exhibiting quasi-one-dimensional (1D) ferromagnetic behavior,[12] while several other derivatives showed a range of different ferromagnetic[13] and antiferromagnetic behaviors.[14] As such the verdazyls offer a fertile source of "structure−magnetism correlations" that help unravel how the molecular structure and solid state packing affects intermolecular magnetic interactions.

Owing to the interest in neutral organic radicals composed only of light elements,[15] the search for new radical families, similar to verdazyl, continues to be of interest. The 1,2,4-benzotriazinyl radicals, first prepared in 1968 by Blatter,[16] are one such class of compounds. 1,3-Diphenyl-1,4-dihydro-1,2,4-benzotriazin-4-yl (**2**) (Blatter's radical) was designed based on the verdazyl radical **1** (Scheme 1). The verdazyl *N*-phenyl substituent was formally benzo-fused across the N5−C6 bond and the bridging N5 atom replaced by C, leading to the benzotriazinyl system.

Relatively few derivatives of Blatter's radical **2** have appeared, though Neugebauer et al.[17] reported a benzotriazinyl radical with short-range antiferromagnetic ordering, which was interpreted in terms of an alternating antiferromagnetic Heisenberg linear chain. The single crystal X-ray structure of Blatter's radical **2** has also been reported.[18] Although in the latter article the authors

Received: January 28, 2011
Published: March 08, 2011

Scheme 1. Structural Relation of Verdazyls and Benzotriazinyls

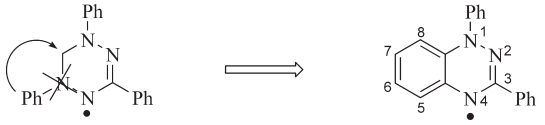

1 2

claim radical **2** to be "super stable", Neugebauer and Umminger showed that when an ethanolic solution of radical **2** was treated with active carbon for 6 weeks under air atmosphere, the radical was oxidized at C7 to give 1,3-diphenyl-1,2,4-benzotriazin-7(1*H*)-one (**3**) in low yield (1%) (Scheme 2).[19]

Oxidation at C5 to give the 1,2,4-benzotriazin-5-one was not observed owing to less spin density at C5 than at C7 consistent with a free-radical mechanism.[19] The stability of the 1,2,4-benzotriazinyl **2** with respect to oxidation at C7 could be improved by introducing a substituent that inhibits oxidation. Many different functional groups have been used to protect spin centers and trifluoromethyl is a good example owing to chemical and oxidative inertness and has been used as a blocking/protecting group for other radicals in the past.[20] Herein, we present the solid state characterization of the 1,3-diphenyl-7-trifluoromethyl-1,4-dihydro-1,2,4-benzotriazin-4-yl (**4**).

RESULTS AND DISCUSSION

Synthesis and Characterizations. The 1,2,4-benzotriazinyl **2** was first prepared by Blatter,[16,21] and later by Huisgen,[22] in low yield *via* the air oxidation of the benzotriazine. Later, Neugebauer and Umminger improved the yield by using HgO to oxidize *N*,*N*′-diphenylbenzenecarbohydrazonamide (*N*-phenylamidrazone).[19,23] We recently developed a gram scale high-yielding (82%) synthesis of Blatter's radical starting from *N*-phenylamidrazone by using catalytic Pd/C and 1,8-diazabicyclo[5.4.0]undec-7-ene (DBU) instead of toxic HgO.[24]

7-Trifluoromethyl benzotriazinyl radical **4** was prepared in a similar manner (Scheme 3).[24] The amidrazone **5** was prepared according to literature protocol[18,25d] *via* treatment of the *N*′-phenylbenzohydrazonoyl chloride with the 4-trifluoromethylaniline. Treating the amidrazone **5** with catalytic Pd/C (1.6 mol %) and DBU (0.1 equiv) at *ca.* 20 °C in air afforded the radical in 80% yield.[24]

Thermal and Oxidative Stability. The thermal stability of the 7-trifluoromethylbenzotriazinyl **4** was comparable to that of Blatter's radical **2**. Both radicals were thermally stable in refluxing benzene (bp 80 °C) and chlorobenzene (bp 131 °C) solutions, and DSC studies identified that decomposition occurred significantly above their melting points. The Blatter radical **2** (mp 111−112 °C) has a decomposition onset at 269 °C, and radical **4** (mp 160−161 °C) suffered a decomposition onset at 288 °C (Figure 1).

The oxidative stability of the radicals was investigated using either MnO_2 or $KMnO_4$ as oxidants. Blatter's radical **2** treated with MnO_2 (10 equiv) in CH_2Cl_2 at *ca.* 20 °C for 7 d or with $KMnO_4$ (10 equiv) in refluxing PhH for 2 d gave the benzotriazinone **3** in 84% and 62% yields, respectively. Conversely, when the 7-trifluoromethylbenzotriazinyl **4** was treated with 10 equiv of either MnO_2 or $KMnO_4$ in CH_2Cl_2 at *ca.* 20 °C and 10 equiv of $KMnO_4$ in refluxing PhH for 2 d, no new products

Scheme 2. Oxidation of Blatter's Radical 2

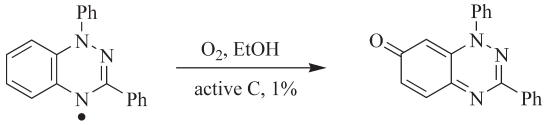

2 3

were observed (by TLC) and the starting radical was recovered unchanged. Blocking the C7 position with a trifluoromethyl group therefore successfully led to significantly greater oxidative stability than the parent Blatter radical.

X-ray Studies. To the best of our knowledge only two crystal structures of benzotriazinyl radicals have been reported: Blatter's radical 1,3-diphenylbenzotriazinyl **2** and 1-(4-chlorophenyl)-3-phenyl-1,2,4-benzotriazinyl **6**.[17a,18] Suitable single crystals of the 7-trifluoromethyl-benzotriazinyl **4** for single crystal X-ray diffraction studies (Table 1) were obtained by slow evaporation of a concentrated hexane solution.

In contrast to the previously reported radicals **2** and **6**, the 1,2,4-amidrazonyl moiety in radical **4** was not planar with a deviation from planarity *ca.* 14.5° as defined by the angle measured between the plane of the N1, N2, C1, N3 amidrazonyl atoms and the plane of the fused phenyl ring (Figure 2). Furthermore, the distance of atom N1 from the plane defined by C1, C2, C7, N1, N2, N3 (0.0795 Å) was larger than those of the other five atoms of this plane. Although the amidrazonyl moiety deviated from planarity, it was far from the *boat* conformations normally adopted by 1,4-dihydro 1,2,4-triazine derivatives.[26]

The strong conjugation in the amidrazonyl moiety of the heterocycle, due to delocalization of the unpaired electron, is reflected in C−N bond lengths [C1−N2, 1.336(2) Å; C1−N3, 1.338(2) Å], which are intermediate between typical single (1.426 Å) and double (1.281 Å) C−N bonds.[27] The C1−N2−N1 and C1−N3−C2 angles in the amidrazonyl moiety were 115.9(1)° and 114.8(2)°, respectively, and were typical of sp^2 hybridized pyridine coordination complexes.[26,28]

The torsion angle (C13, C8, N1, N2) of the *N*-phenyl group with respect to the plane of the benzotriazine (37.7°) was smaller than the corresponding angle of radical **2** (54°) and radical **6** (56.9°) (Figure 2). While this phenyl substituent does not participate in $\pi-\pi$ contacts, weak intramolecular contact between the H13 atom of the phenyl ring and the N2 atom of the amidrazonyl moiety (C13−H13···N2, 2.78 Å) may help to stabilize its geometry. Steric interactions between the *peri* hydrogen H6 and the phenyl *ortho* hydrogen H9 presumably inhibit the phenyl ring from adopting a coplanar geometry with the benzotriazinyl ring. In contrast the phenyl substituent at C1, where there are no such steric clashes with functionalities in the *ortho* positions, was almost coplanar with the amidrazonyl plane (N1, N2, C1, N3). Two favorable but weak intramolecular C−H···N contacts (C15−H15···N2, 2.79 Å; C19−N19···N3, 2.81 Å) may account for the observed C1 phenyl's torsion angle (C19, C14, C1, N3) of 16.1°, which was slightly bigger than the corresponding angle in radical **2** (8°) but about the same as in radical **6** (15.9°).

The presence of close intermolecular contacts between radicals in the solid state (significantly shorter than the sum of the van der Waals radii) often reflect strong bonding interactions between radical centers, e.g., formation of singlet ground state

dx.doi.org/10.1021/jo200210s |*J. Org. Chem.* 2011, 76, 2798–2806

Scheme 3. Synthetic Route to 7-Trifluoromethylbenzotriazinyl Radical 4

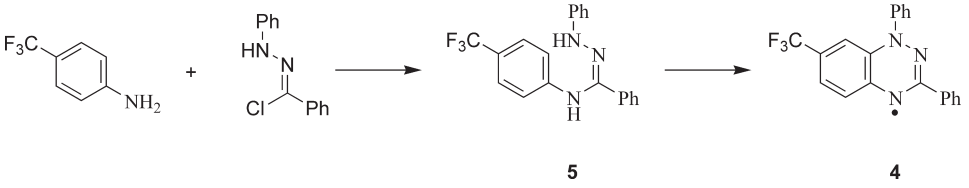

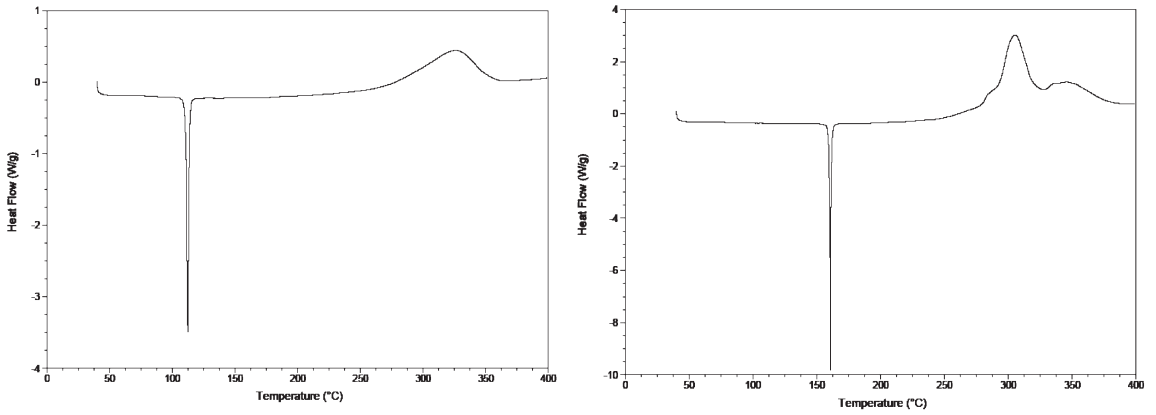

Figure 1. DSC of 1,2,4-benzotriazinyls **2** and **4** with a heating curve from 40−400 °C under Ar atmosphere (heating rate 5 °C/min).

Table 1. Crystallographic Data for Compound 4

Crystal Data	
formula	$C_{20}H_{13}F_3N_3$
formula weight, g mol^{-1}	352.33
crystal system	orthorhombic
space group	$Pca2_1$
a, b, c, Å	7.6398(2), 10.5667(3), 19.3868(5)
V, Å^3	1565.05(7)
Z	4
ρ_{calc}, g cm^{-3}	1.495
μ(Mo Ka), mm^{-1}	0.115
F(000)	724
crystal size, mm^3	0.2 × 0.08 × 0.02
Data Collection	
T, K	100(2)
λ^a, Å	0.71073
θ (min, max), deg	3.45, 29
data set ($-h$, h; $-k$, k; $-l$, l)	−10, 10; −14, 14; −26, 19
meas/indep refl (R_{int})	13059/2142 (0.0229)
obs refl [$I > 2\sigma(I)$].	1945
Refinement	
$R_1{}^b$	0.0285
$wR_2{}^c$	0.0716
goodness of fit on F^2	1.093
min, max resd density, e Å^{-3}	0.219/ −0.145

[a] Graphite monochromator. [b] $R_1 = \Sigma||F_o| - |F_c||/\Sigma|F_o|$. [c] $wR_2 = [\Sigma[w(F_o^2 - F_c^2)^2]/\Sigma[wF_o^2)^2]]^{1/2}$, $w = 1/[\sigma^2(F_o^2) + (m\cdot p)^2 + n\cdot p]$, $p = [\max(F_o^2,0) + 2F_c^2]/3$.

configurations in $(TCNE)_2{}^{2-}$ or $(ArCNSSN)_2$ $\pi^*-\pi^*$ dimers,[6,29] or formation of σ-bonded dimers, e.g., in phenalenyl.[30] Since the majority of the spin density resides on the triazinyl ring, then the close contacts between triazinyl heterocycles were considered important for an understanding of the magnetic behavior. A careful examination of the packing revealed that radical **4** forms slipped π-stacks along the a axis (Figure 3a) with a slippage angle of 27.8°. Within these π-stacks the heterocyclic rings (Figure 3b) formed a regular set of long contacts greater than the sum of the van der Waals radii, consistent with retention of their paramagnetic nature in the solid state. For example, the distance between the N3 atoms of neighboring π-stacked radicals (N3···N3′, 3.82 Å in Figure 3b) was well above the sum of their van der Waals radii (3.1 Å). Radical **4** appeared to be stable toward Peierls distortion in contrast to radical **6**, which packed in columns of radicals with alternating long and short distances forming discrete dimers.[17a] The radicals within the columns are related by an inversion center, thereby minimizing steric repulsion of the CF_3 groups as well as the phenyls (Figure 3b) in relation to the packing direction.

Covalently bound fluorine hardly ever acts as a strong hydrogen bond acceptor.[31] While the interactions between heavier halogens can be considered attractive, the F···F attractive interactions are weaker owing to the hard nonpolarizable nature of the F atoms.[32] Furthermore, the small size of F means that the repulsive interactions between F atoms only become important at a very close range. Since there are neither strong attractive nor repulsive forces the interactions are nonbonding, and often it appears that F atoms act merely as "space fillers" within crystal structures.[32]

In the structure of radical **4**, neighboring columns are connected through a net of contacts including some in which the CF_3

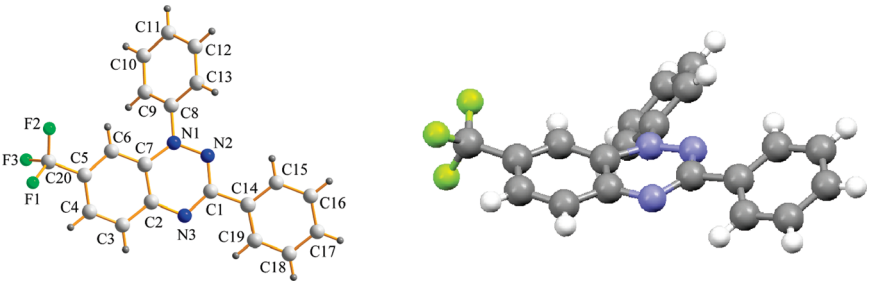

Figure 2. Geometry of radical **4** in the crystal and the crystallographic atom numbering that is used in the discussion of the X-ray structure, which differs from IUPAC.

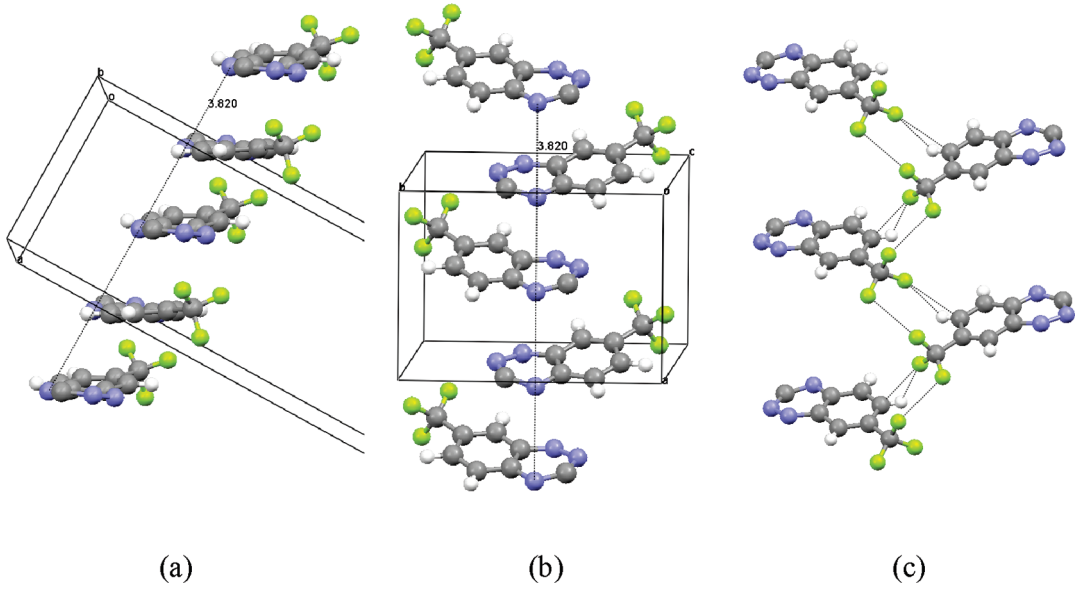

Figure 3. Diagrams of radical **4** showing the packing along the *a* axis. The phenyl rings are omitted for clarity reasons.

groups participate (Figure 3c); these weak intercolumn C−H···F−C contacts (2.62−2.67 Å) appear to link adjacent radicals in a head-to-tail manner parallel to *c* and are related *via* a 2_1 screw axis. Even longer C−F···H−C contacts to the N-bound phenyl group generate 2D sheets in the *bc* plane (Figure 4a). The sheets pack in a parallel zigzag arrangement down the *a* axis (Figure 4b), giving rise to efficient packing without any voids potentially accessible to solvent molecules. The closest F···F contacts between CF_3 groups (2.92 Å) falls close to the sum of van der Waals radii (2.94 Å). Similar contacts and distances between CF_3 groups have also been observed in the crystal design of 1,4-diphenyl-1,3-butadienes for topochemical [2 + 2] photodimerizations where CF_3 groups have been used as steering devices.[33]

Cyclic Voltammetry and EPR Spectroscopy. The electrochemical behavior of a 1 mM CH_2Cl_2 solution of radical **4** has been probed by cyclic voltammetry using *n*-Bu_4NPF_6 as supporting electrolyte (Figure 5). The results are presented in the form of half-wave potentials $E_{1/2}$ (Table 2) along with the values for the isoelectronic benzothiadiazinyls **7** and **8**. Radical **4** showed two fully reversible waves, corresponding to the −1/0 and 0/+1 processes. With a ${E_{1/2}}^{0/+1}$ of +0.36 V, radical **4** was more stable toward oxidation than Blatter's radical **2** but did not reach the stability of the 1,2,4-benzothiadiazinyls **7** and **8** with a ${E_{1/2}}^{0/+1}$ of 1.20 V.[20a] Indeed the redox potential of radical **4** indicates that it is comparable with the electron donor TTF (${E_{1/2}}^{0/+1}$ = 0.30 V). Interestingly, an organic charge transfer salt between Blatter's radical (**2**) and TCNQ has previously been reported and was a semiconductor with a pressure-dependent conductivity.[34]

The reduction potential of radical **4** was marginally smaller than the corresponding value of Blatter's radical **2** but was more stable toward reduction than the benzothiadiazinyls **7** and **8**. While the benzothiadiazinyls reduce easily to give benzothiadiazines, the benzotriazinyls are protonated only under reducing conditions e.g., in phenylhydrazine and are rapidly oxidized in air back to the radical.

Previous EPR studies on the Blatter radical **2**, the 1-(4-chlorophenyl) **6** and the 3-*tert*-butyl derivative **9** showed that the spin density was mainly delocalized on the amidrazonyl fragment of the 1,2,4-triazinyl cycle.[17a,19,22,25] The largest hyperfine coupling constant is observed on the N1 atom (∼7.5 G), whereas the N2 and N4 coupling constants are smaller and approximately equal to each other (∼5.1 G). These two coupling constants were separately measured with further EPR studies on deuterated derivatives of the 3-*tert*-butyl benzotriazinyl **9** and found to be 4.9 G for N2 and 5.2 G for N4.[23] The coupling constants of the N-Ph and C-Ph ring protons were an order of magnitude smaller.[25d] The EPR spectrum of radical **4** (Figure 6) was measured at *ca.* 20 °C and simulated to find a *g* value of 2.0036 similar to that of radical **2** (2.0033).

The EPR spectrum shows coupling not only to the N atoms of the 1,2,4-amidrazonyl moiety $a_N(1)$ = 7.62, $a_N(2)$ = 4.95 and

dx.doi.org/10.1021/jo200210s |*J. Org. Chem.* 2011, 76, 2798–2806

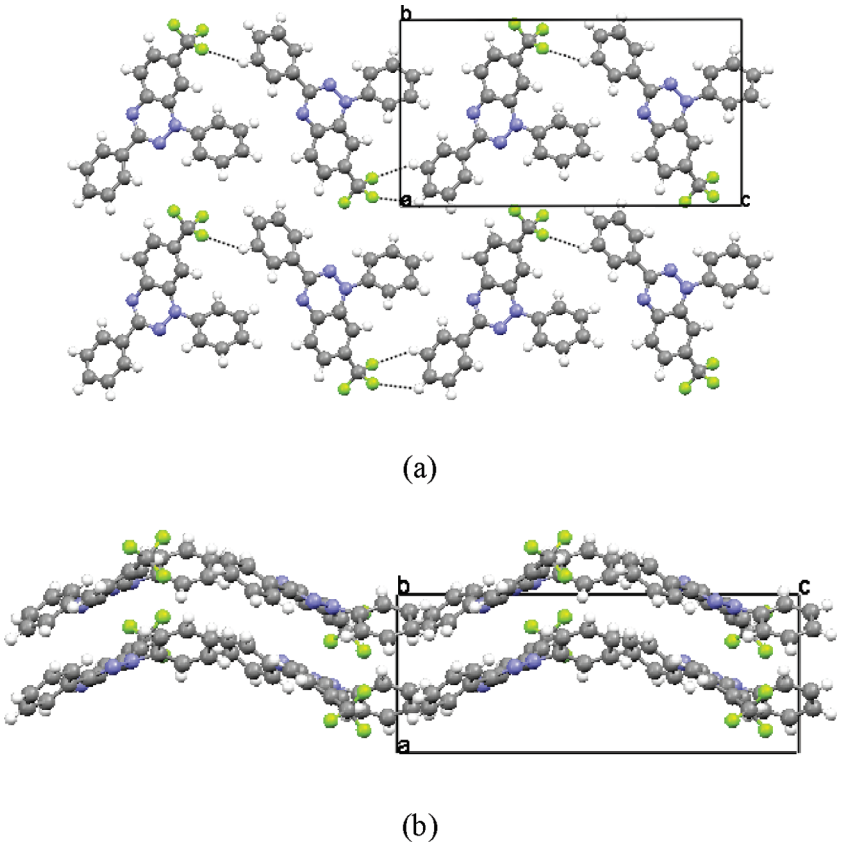

Figure 4. Diagrams of radical **4** showing the packing along the *c* axis.

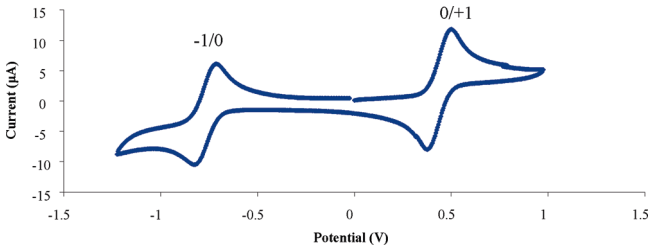

Figure 5. Cyclic voltammogram of the 7-trifluoromethylbenzotriazinyl **4** (1 mM), *n*-Bu_4NPF_6 0.1 M, 50 mV/s.

$a_N(3)$ = 4.56 G but also to the three equivalent F atoms of the CF_3 group a_F = 3.46 G. Fluorine has a particularly large atomic hyperfine parameter,[35] and so hyperfine coupling to F does not represent large spin density at F. Indeed DFT calculated spin densities at the UB3LYP/6-311+G(d,p) level confirm the majority of spin density resides on the triazinyl ring with the highest spin density almost evenly distributed between N2 and N3. Estimates of spin density distributions in organic radicals rely on McConnell's estimates of the spin density at C (ρ_C) through a linear relationship with the hyperfine coupling constant to the H bonded to it (A_H):[36]

$$A_H = Q_H\rho_C \quad (1)$$

where A_H is the hyperfine coupling constant in Gauss and Q_H = (−)27.3 G.[36] A number of groups have extended this approach to estimate the spin density at N (eq 2) from its hyperfine coupling constant, but this appears sensitive to the nature of the N atom. When the N is sp^2 hybridized with a lone pair, values for Q_N are typically given in the region of 53−59 MHz.[37]

$$A_N = Q_N\rho_N \quad (2)$$

We have implemented polarized neutron diffraction data and EPR data on the organic radical *p*-$O_2NC_6F_4CNSSN$[38] to estimate an appropriate value of Q_N that is consistent with experimentally

Table 2. Cylic Voltammetry Data of 1,2,4-Benzotriazinyl and 1,2,4-Benzothiadiazinyl Radicals[a]

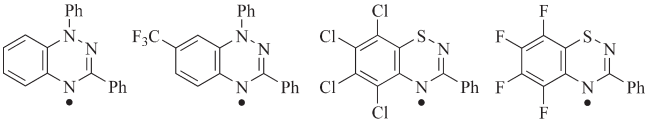

2 **4** **7** **8**

radical	$E_{1/2}^{0/+1}$	$E_{1/2}^{-1/0}$	E_{cell}[b]
2[c]	0.10	−0.96	1.06
4[a]	0.36	−0.84	1.20
7[d]	1.20[e]	−0.04	1.24
8[d]	1.20[e]	−0.11	1.31

[a] The concentrations of radical **4** used was 1 mM in CH_2Cl_2. A 0.1 M CH_2Cl_2 solution of *n*-Bu_4NPF_6 was used as the electrolyte. The reference electrode was Ag/AgCl, and the scan rate was 50 mV/s. Ferrocene was used as an internal reference. [b] $E_{cell} = E_{1/2}^{0/+1} - E_{1/2}^{-1/0}$. [c] Reference 34. [d] Reference 20a. [e] Oxidation is irreversible.

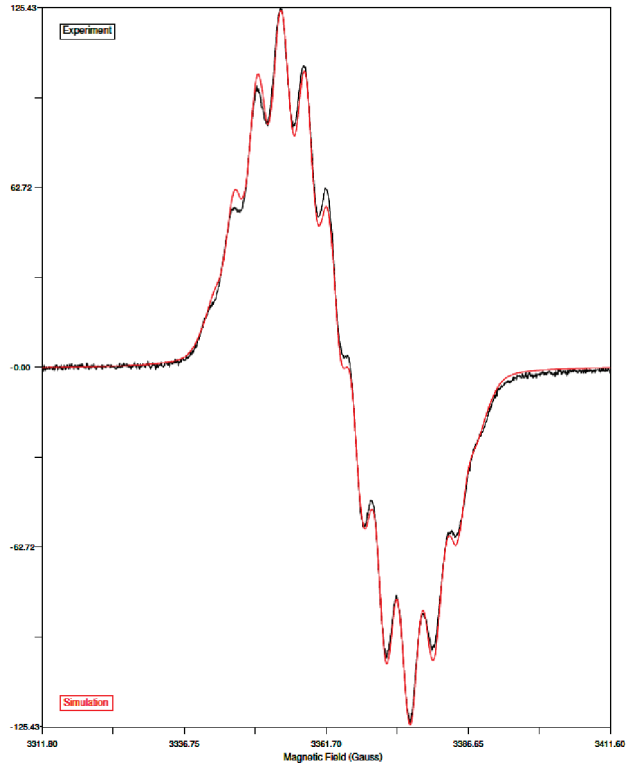

Figure 6. Experimental and simulated EPR spectrum of radical **4** at rt in CH_2Cl_2. Fitting parameters: g = 2.0036, $a_N(1)$ = 7.62, $a_N(2)$ = 4.95, $a_N(3)$ = 4.56, a_F = 3.46 G (3 equivalent F) (Lineshape: ΔH_{pp} = 2.17 G; 45% Lorentzian, 55% Gaussian).

determined spin density data. This gives Q_N = 59.28 MHz, at the upper end of the previously cited range. Using this value we estimate the spin density at N2 and N3 to be ∼22−23%. When the sp^2-N atom bears a substituent, then the value of Q_N is substantially larger (∼70 MHz).[37] Using this value the experimental spin density at N1 is therefore likely to be a little larger than at N2 and N3. This confirms the majority of spin density to be located on the triazinyl ring with the largest component of the spin density residing on N1 (Table 3) in accordance with the previous observations.[17a,19,22,25]

Magnetic Properties. Although both the syntheses and EPR studies on benzotriazinyls have been well documented, studies of the magnetic properties are few. To our knowledge only one report has been published on the magnetic behavior of these radicals and describes the magnetic properties of the Blatter radical **2**, the 1-(4-chlorophenyl)-3-phenyl-1,2,4-benzotriazinyl **6** and the 3-*tert*-butyl-1-phenyl-1,2,4-benzotriazinyl **9**.[17a]

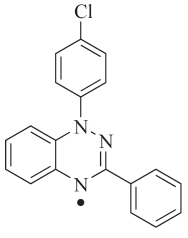

6

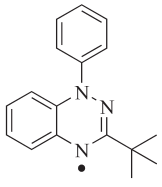

9

Magnetic susceptibility measurements on radicals **2** and **9** showed a Curie−Weiss paramagnetic behavior with a negative

Table 3. Spin Densities Estimated from Hyperfine Coupling Constants and DFT Calculations for Radical 4

	ρ	
	EPR	DFT
$a_N(1)$	0.305	0.226
$a_N(2)$	0.234	0.334
$a_N(3)$	0.216	0.315

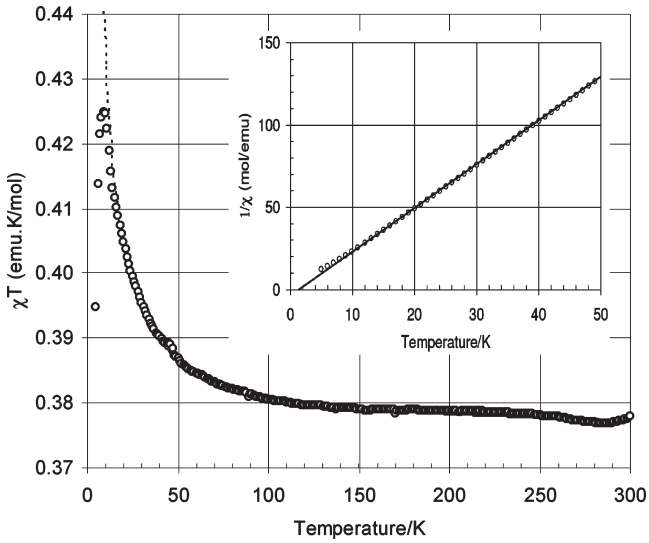

Figure 7. Temperature dependence of χT for radical **4**. The dashed line represents the best fit to the one-dimensional Heisenberg linear chain model (g = 2.00, J/k = +1.49 K; see text for details). Inset Curie−Weiss behavior in the low temperature region (C = 0.376, θ = +1.41 K).

Weiss constant of −2.2 and −0.3 K, respectively, indicative of very weak antiferromagnetic communication between radical centers. Conversely, the magnetic susceptibility of radical **6** exhibits a broad maximum at 142 K characteristic of short-range or low dimensional antiferromagnetic ordering with very efficient communication. This susceptibility was interpreted in terms of an alternating antiferromagnetic Heisenberg linear chain model with an exchange interaction of $2J_1/k$ = −220 K and an alternation parameter of $a = J_2/J_1$ = 0.3.

In light of these results we recorded the variable temperature magnetic susceptibility of the 7-trifluoromethyl benzotriazinyl **4** in the region 5−300 K and in an applied magnetic field of 5000 G. The data were corrected for both sample diamagnetism (Pascal's constants) and the diamagnetism of the sample holder. The compound obeyed Curie−Weiss behavior down to 10 K with C = 0.376 emu·K·mol^{-1} expected for an S = 1/2 paramagnet (g = 2.0036) and θ = +1.41 K, consistent with weak ferromagnetic interactions between radicals (Figure 7, inset). The increase of χT upon cooling in the plot of χT vs T reveals the presence of ferromagnetic interactions between spins in a benzotriazinyl radical for the first time. The close π-stacked arrangement of molecules parallel to the crystallographic a-axis suggested that the magnetic behavior may best be interpreted in terms of a one-dimensional Heisenberg ferromagnetic chain model. With each molecule in the chain possessing two symmetry equivalent nearest neighbors related *via* a 2_1 screw axis

dx.doi.org/10.1021/jo200210s |*J. Org. Chem.* 2011, 76, 2798–2806

$(x - 1/2, 1 - y, z)$, the regular Heisenberg ferromagnetic chain model using the Hamiltonian in eq 3 was employed.[39] The exchange constant J is the intrachain exchange constant between neighboring molecules i and j.

$$H = -2J\sum S_i \cdot S_j \quad (3)$$

Analytical solutions for the magnetic susceptibility of such regular Heisenberg 1D chains have been reported including the high-temperature series expansion (eq 4).[40]

$$\chi = \frac{Ng^2\beta^2}{4kT}\left[\frac{A}{B}\right]^{2/3} \quad (4)$$

where $A = 1.0 + 5.7979916y + 16.902653y^2 + 29.376885y^3 + 29.832959y^4 + 14.036918y^5$; $B = 1.0 + 2.7979916y + 7.0086780y^2 + 8.6538644y^3 + 4.5743114y^4$; and $y = J/2kT$.

A first estimate of J from the mean field approximation yielded $J/k = \theta = +1.41$ K. Subsequent fitting of the magnetic data to the 1D ferromagnetic chain model (eq 4) provided an excellent fit ($g = 2.00$, $J/k = +1.49$ K) down to 10 K but failed to reproduce the subsequent decrease in χT at low temperatures. This deviation from ideal 1D behavior heralds the onset of weak antiferromagnetic interchain interactions at low temperatures, leading to higher dimensionality. For a Heisenberg spin (appropriate for organic radicals such as benzotriazinyl **4** with small single ion anisotropy) the long-range magnetic order is only observed when the interactions propagate in all three dimensions.[25] 1D ferromagnetic interactions have been observed in other classes of organic radicals such nitronyl nitroxides[3] and verdazyls,[12] but this is the first time observed with benzotriazinyls.

CONCLUSIONS

Despite the reasonable thermal and air stability of the 1,2,4-benzotriazinyl radicals, oxidation can occur at C7, resulting in the loss of the radical electronic structure and the formation of the analogous quinonimine **3**. In this paper we have demonstrated that introduction of a CF_3 group at the C7 position can lead to exceptional oxidative stability. 1,3-Diphenyl-7-trifluoromethyl-1,4-dihydro-1,2,4-benzotriazinyl (**4**) was treated with $KMnO_4$ (10 equiv) in refluxing benzene for 2 d and was recovered unchanged. Unlike previously reported benzotriazinyls, magnetic studies on radical **4** reveal the presence of a dominant ferromagnetic exchange interaction, which is tentatively assigned to the regular stacking of radicals parallel to the crystallographic a-axis. Elegant studies by Oakley on heavier p-block radicals have shown that the nature of the magnetic exchange along the π-stacking direction is sensitive to the degree of slippage.[6b] In the current system weak antiferromagnetic interactions between the neighboring stacks quenches the potential for bulk ferromagnetism at low temperature. Further modifications to the benzotriazinyl framework are in progress.

EXPERIMENTAL SECTION

General Synthetic Methods. Radicals **2** and **4** were prepared according to literature procedures.[24] 1,3-Diphenyl-1,2,4-benzotriazin-7(1*H*)-one (**3**) was prepared by the oxidation of the 1,3-diphenyl-1,2,4-benzotriazinyl **2** using either MnO_2 or $KMnO_4$ as oxidants.

1,3-Diphenyl-1,2,4-benzotriazin-7(1*H*)-one (3). *(A) MnO_2 Method.* To a stirred solution of 1,3-diphenyl-1,2,4-benzotriazinyl **2** (51 mg, 0.18 mmol) in CH_2Cl_2 (2.5 mL) was added MnO_2 (153 mg, 1.76 mmol), and the mixture stirred at *ca.* 20 °C for 7 d. The mixture was then diluted with CH_2Cl_2 (30 mL), adsorbed onto silica gel and dry flash chromatographed (*t*-BuOMe/hexane, 1:4 → *t*-BuOMe) to give the title compound **3** (45 mg, 84%) as purple needles, mp 215−218 °C (lit.[24] 215−218 °C) (benzene), identical to an authentic sample.

(B) $KMnO_4$ Method. To a stirred solution of 1,3-diphenyl-1,2,4-benzotriazinyl **2** (51 mg, 0.18 mmol) in PhH (2 mL) was added $KMnO_4$ (280 mg, 1.77 mmol) was added, and the mixture was refluxed for 2 d. The mixture was then diluted with CH_2Cl_2 (30 mL), adsorbed onto silica gel and dry flash chromatographed (*t*-BuOMe/hexane, 1:4 → *t*-BuOMe) to give the title compound **3** (33 mg, 62%) as purple needles, mp 215−218 °C (lit.,[24] 215−218 °C) (benzene), identical to an authentic sample.

Instrumental Analyses. Differential scanning calorimetric (DSC) measurements were performed on a DSC TA Q1000 apparatus using a heating curve from 40 to 400 °C, under argon atmosphere with a heating rate of 5 °C/min. The samples (0.8−1.5 mg) were measured in hermetically sealed aluminum pans. Cyclic voltammetry (CV) measurements were performed on a Princeton Applied Research Potentiostat/Galvanostat 263A apparatus. The concentrations of the benzotriazinyl radicals used were 1 mM in CH_2Cl_2. A 0.1 M CH_2Cl_2 solution of tetrabutylammonium hexafluorophosphate ($TBAPF_6$) was used as electrolyte. The reference electrode was Ag/AgCl and the scan rate was 50 mV/s. Ferrocene was used as an internal reference; the $E_{1/2}$(ox) of ferrocene in this system was 0.352 V.[41] Electron paramagnetic resonance (EPR) measurements were carried out on a Bruker EMX spectrometer using an X-Band (9.8 GHz) microwave bridge at 290 K. The EPR spectrum was simulated using the Winsim Spectral Simulation for MS-Windows 9x, NT v0.98.[42] Magnetic susceptibility measurements were performed on a Quantum Design MPMS-XL SQUID magnetometer in the temperature region of 5−300 K and in an applied magnetic field of 5000 G. X-ray diffraction data were collected on an Oxford-Diffraction diffractometer, equipped with a CCD area detector and a graphite monochromator utilizing Mo K_α radiation (λ = 0.71073 Å). A suitable crystal was attached to a glass fiber using paratone-N oil and transferred to a goniometer where it was cooled for data collection using an Oxford Instruments cryostream. Unit cell dimensions were determined and refined by using 7879 ($3.45° < \theta < 30.49°$), reflections. Empirical absorption corrections (multiscan based on symmetry-related measurements) were applied using CrysAlis RED software.[43] The structures were solved by direct methods using SIR92,[44a] and refined on F^2 using full-matrix least-squares using SHELXL97.[44b] Programs used: CrysAlis CCD[43] for data collection, CrysAlis RED[40] for cell refinement and data reduction, and DIAMOND[45a] and MERCURY[45b] for molecular graphics. The non-H atoms were treated anisotropically, whereas the hydrogen atoms were placed in calculated, ideal positions and refined using a riding model. Unit cell data and structure refinement details are listed in Table 1. Full details can be found in the CIF file provided in the Supporting Information.

Computational Methods. Single-point calculations using the UB3LYP level of theory with the higher level basis set of 6-311+G(d,p) were carried out on the X-ray geometry of radical **4** to calculate the spin density distributions. The above computation was performed using the Gaussian 03 suite of programs.[46]

ASSOCIATED CONTENT

Supporting Information. Complete crystallographic summary of 1,3-diphenyl-7-trifluoromethyl-1,4-dihydro-1,2,4-benzotriazin-4-yl (**4**) in CIF format. This material is available free of charge via the Internet at http://pubs.acs.org.

NOTE ADDED IN PROOF

While this manuscript was under review other related benzotriazinyl radicals were also reported: [a] Yan, B.; Cramen, J.;

McDonald, R.; Frank, N. L. *Chem. Commun.* **2011**, *47*, 3201–3203. b) Constantinides, C.P.; Koutentis, P.A.; Loizou, G. *Org. Biomol. Chem.* **2011**, DOI: 10.1039/C1OB05167A].

AUTHOR INFORMATION

Corresponding Author
*E-mail: koutenti@ucy.ac.cy.

ACKNOWLEDGMENT

The authors wish to thank the University of Cyprus (Medium Sized Grants) for supporting H.K., the Cyprus Research Promotion Foundation [grant no. ΥΓΕΙΑ/ΒΙΟΣ/0308(ΒΙΕ)/13] and the following organizations in Cyprus for generous donations of chemicals and glassware: the State General Laboratory, the Agricultural Research Institute, the Ministry of Agriculture and Biotronics Ltd. Furthermore, we thank the A. G. Leventis Foundation for helping to establish the NMR facility in the University of Cyprus.

REFERENCES

(1) (a) *Magnetic Properties of Organic Materials*; Lahti, P. M., Ed.; Marcel-Dekker Inc.: New York, 1999. (b) *Molecular Magnetism: New Magnetic Materials*; Itoh, K., Kinoshita, M., Ed.; Kodansha and Gordon & Breach: Tokyo, Amsterdam, 2000.

(2) Nakatsuji, S.; Anzai, H. *J. Mater. Chem.* **1997**, *7*, 2161–2174.

(3) (a) Kamachi, M.; Sugimoto, H.; Kajiwara, A.; Harada, A.; Morishima, Y.; Mori, W.; Ohmae, N.; Nakano, M.; Sorai, M.; Kobayashi, T.; Amaya, K. *Mol. Cryst. Liq. Cryst.* **1993**, *232*, 53–60. (b) Ishida, T.; Tomioka, K.; Nogami, T.; Iwamura, H.; Yamaguchi, K.; Mori, W.; Shirota, Y. *Mol. Cryst. Liq. Cryst.* **1993**, *232*, 99–102. (c) Murata, H.; Miyazaki, Y.; Inaba, A.; Paduan-Filho, A.; Bindilatti, V.; Oliveira, N. F., Jr.; Delen, Z.; Lahti, P. M. *J. Am. Chem. Soc.* **2008**, *130*, 186–194.

(4) (a) Chouteau, G.; Veyret-Jeandey, C. *J. Phys. (Paris)* **1981**, *42*, 1441–1444. (b) Nogami, T.; Togashi, K.; Tsuboi, H.; Ishida, T.; Yoshikawa, H.; Yasui, M.; Iwasaki, F.; Iwamura, H.; Takeda, N.; Ishikawa, M. *Synth. Met.* **1995**, *71*, 1813–1814.

(5) (a) Tamura, M.; Nakazawa, Y.; Shiomi, D.; Nozawa, K.; Hosokoshi, Y.; Ishikawa, M.; Takahashi, M.; Kinoshita, M. *Chem. Phys. Lett.* **1991**, *186*, 401–404. (b) Mito, M.; Kawae, T.; Ikegami, A.; Hitaka, M.; Takeda, K.; Nakatsuji, S.; Morimoto, H.; Anzai, H. *Phys. B* **2000**, *284*, 1493–1494. (c) Mito, M.; Kawae, T.; Hitaka, M.; Takeda, K.; Ishida, T.; Nogami, T. *Chem. Phys. Lett.* **2001**, *333*, 69–75.

(6) (a) Rawson, J. M.; Alberola, A.; Whalley, A. *J. Mater. Chem.* **2006**, *16*, 2560–2575. (b) Mito, M.; Komorida, Y.; Tsuruda, H.; Tse, J. S.; Desgreniers, S.; Ohishi, Y.; Leitch, A. A.; Cvrkalj, K.; Robertson, C. M.; Oakley, R. T. *J. Am. Chem. Soc.* **2009**, *131*, 16012–16013. (c) Robertson, C. M.; Leitch, A. A.; Cvrkalj, K.; Myles, D. J. T.; Reed, R. W.; Dube, P. A.; Oakley, R. T. *J. Am. Chem. Soc.* **2008**, *130*, 14791–14801. (d) Leitch, A. A.; Brusso, J. L.; Cvrkalj, K.; Reed, R. W.; Robertson, C. M.; Dube, P. A.; Oakley, R. T. *J. Chem. Soc., Chem. Commun* **2007**, 3368–3370.

(7) Rajca, A. *Chem. Rev.* **1994**, *94*, 871–893.

(8) Hicks, R. G. *Org. Biomol. Chem.* **2007**, *5*, 1321–1338.

(9) (a) Kuhn, R.; Trischmann, H. *Angew. Chem., Int. Ed.* **1963**, *2*, 155. (b) Nineham, A. W. *Chem. Rev.* **1955**, *55*, 355–483. (c) Neugebauer, F. A.; Fischer, H. *Angew. Chem., Int. Ed.* **1980**, *19*, 724–725. (d) Neugebauer, F. A.; Fischer, H.; Siegel, R. *Chem. Ber.* **1988**, *121*, 815–822. (e) Neugebauer, F. A.; Fischer, H. *J. Chem. Soc., Perkin Trans.* **1981**, *2*, 896–900. (f) Neugebauer, F. A.; Fischer, H.; Krieger, C. *J. Chem. Soc., Perkin Trans.* **1993**, *2*, 535–544. (g) Katritzky, A. R.; Belyakov, S. A. *Synthesis* **1997**, 17–19.

(10) Koivisto, B. D.; Hicks, R. G. *Coord. Chem. Rev.* **2005**, *249*, 2612–2630.

(11) Azuma, N.; Yamauchi, J.; Mukai, K.; Ohyanish, H.; Degushi, Y. *Bull. Chem. Soc. Jpn.* **1973**, *46*, 2728–2734.

(12) (a) Allemand, P.-M.; Srdanov, G.; Wudl, F. *J. Am. Chem. Soc.* **1990**, *112*, 9391–9392. (b) Allemand, P.-M.; Srdanov, G.; Wudl, F. *Synth. Met.* **1991**, *43*, 3245–3248. (c) Mito, M.; Takeda, K.; Mukai, K.; Azuma, M.; Gleiter, M. R.; Krieger, C.; Neugebauer, F. A. *J. Phys. Chem. B* **1997**, *101*, 9517–9524. (d) Mukai, K.; Nuwa, M.; Suzuki, K.; Nagaoka, S.; Achiwa, N.; Jamali, J. B. *J. Phys. Chem. B* **1998**, *102*, 782–787.

(13) (a) Mukai, K.; Nedachi, K.; Jamali, J. B.; Achiwa, N. *Chem. Phys. Lett.* **1993**, *214*, 559–562. (b) Mukai, K.; Konishi, K.; Nedachi, K.; Takeda, K. *J. Magn. Magn. Mater.* **1995**, *140*, 1449–1550. (c) Mukai, K.; Kawasaki, S.; Jamali, J. B.; Achiwa, N. *Chem. Phys. Lett.* **1995**, *241*, 618–622. (d) Mukai, K.; Konishi, K.; Nedachi, K.; Takeda, K. *J. Phys. Chem.* **1996**, *100*, 9658–9663.

(14) (a) Kremer, R. K.; Kanellakopulos, B.; Bele, P.; Brunner, H.; Neugebauer, F. A. *Chem. Phys. Lett.* **1994**, *230*, 255–259. (b) Hicks, R. G.; Lemaire, M. T.; Ohrstrom, L.; Richardson, J. F.; Thompson, L. K.; Xu, Z. Q. *J. Am. Chem. Soc.* **2001**, *123*, 7154–7159. (c) Mukai, K.; Azuma, N.; Ishizu, K. *Bull. Chem. Soc. Jpn.* **1970**, *43*, 3618–3619. (d) Brook, D. J. R.; Fox, H. H.; Lynch, V.; Fox, M. A. *J. Phys. Chem.* **1996**, *100*, 2066–2071. (e) Azuma, N.; Deguchi, Y.; Marumo, F.; Saito, Y. *Bull. Chem. Soc. Jpn.* **1975**, *48*, 825–829. (f) Dorman, E.; Winter, H.; Dyakonow, W.; Gotschy, B.; Lang, A.; Naarman, H.; Walker, N.; Bunsen-Ges, B. *Phys. Chem. Chem. Phys.* **1992**, *96*, 922–930.

(15) Miller, J. S.; Epstein, A. J. *Angew. Chem., Int. Ed.* **1994**, *33*, 385–415.

(16) Blatter, H. M.; Lukaszewski, H. *Tetrahedron Lett.* **1968**, *9*, 2701–2705.

(17) (a) Mukai, K.; Inoue, K.; Achiwa, N.; Jamali, J. B.; Krieger, C.; Neugebauer, F. A. *Chem. Phys. Lett.* **1994**, *224*, 569–575. (b) Krieger, C.; Neugebauer, F. A. *Acta Crystallogr.* **1996**, *C52*, 3124–3126.

(18) Gubaidullin, A. T.; Buzykin, B. I.; Litvinov, I. A.; Gazetdinova, N. G. *Russ. J. Gen. Chem.* **2004**, *74*, 939–943.

(19) Neugebauer, F. A.; Umminger, I. *Chem. Ber.* **1980**, *113*, 1205–1225.

(20) (a) Zienkiewicz, J.; Kaszynksi, P. *J. Org. Chem.* **2004**, *69*, 7525–7536. (b) Alberola, A.; Clarke, C. S.; Haynes, D. A.; Pascu, S. I.; Rawson, J. M. *J. Chem. Soc., Chem. Commun.* **2005**, 4726–4728.

(21) Blatter, H. M. U.S. Patent 3,423,409, 1969.

(22) Huisgen, R.; Wolf, J. *Chem. Ber* **1969**, *102*, 1848–1858.

(23) Neugebauer, F. A.; Umminger, I. *Chem. Ber* **1981**, *114*, 2423–2430.

(24) Koutentis, P. A.; Lo, Re, D. *Synthesis* **2010**, 2075–2079.

(25) (a) Gilchrist, T. L.; Harris, C. J.; Rees, C. W. *J. Chem. Soc., Chem. Commun.* **1974**, 485–486. (b) Kadirov, M. K.; Il'yasov, A. V.; Vafina, A. A.; Buzykin, B. I.; Gazetdinova, N. G.; Kitaev, Yu. P. *Izv. Akad. Nauk. SSSR, Ser. Khim.* **1984**, *33*, 649–650. (c) Neugebauer, F. A.; Rimmler, G. *Magn. Reson. Chem.* **1988**, *26*, 595–600. (d) Kadirov, M. K.; Buzykin, B. I.; Gazetdinova, N. G. *Russ. Chem. Bull.* **2002**, *51*, 1796–1799.

(26) Gainsford, G. J.; Woolhouse, A. D. *Aust. J. Chem.* **1980**, *33*, 2447–2454.

(27) Allen, F. H.; Kennard, O.; Watson, D. G.; Brummer, L.; Orpen, A. G.; Taylor, R. *J. Chem. Soc., Perkin Trans.* **1987**, *2*, S1–S19.

(28) (a) Schmidt, R. R. *Angew. Chem., Int. Ed.* **1975**, *14*, 581–591. (b) Butler, R. N.; Evans, A. M.; McNeela, E. M.; O'Haloran, G. A.; O'Shea, P. D.; Cunningham, D.; McArdle, P. *J. Chem. Soc., Perkin Trans. 1* **1990**, *9*, 2527–2536.

(29) (a) Novoa, J. J.; Lafuente, P.; Del Sesto, R. E.; Miller, J. S. *Angew. Chem., Int. Ed.* **2001**, *40*, 2540–2545. (b) Del Sesto, R. E.; Miller, J. S.; Lafuente, P.; Novoa, J. J. *Chem.—Eur. J.* **2002**, *8*, 4894–4908. (c) Jakowski, J.; Simons, J. *J. Am. Chem. Soc.* **2003**, *125*, 16089–16096.

(30) (a) Sogo, P. B.; Nakazaki, M.; Calvin, M. *J. Chem. Phys.* **1957**, *26*, 1343–1345. (b) Gerson, F. *Helv. Chim. Acta* **1966**, *49*, 1463–1467.

(31) Rosenfield, R. E., Jr.; Parthasarathy, R.; Dunitz, J. D. *J. Am. Chem. Soc.* **1977**, *99*, 4860–4862.

(32) Reichenbächer, K.; Süss, H. I; Hulliger, J. *Chem. Soc. Rev.* **2005**, *34*, 22–30.

(33) Liu, J.; Wendt, N. L.; Boarman, K. J. *Org. Lett.* **2005**, *7*, 1007–1010.

(34) (a) Hutchison, K.; Srdanov, G.; Menon, R.; Gabriel, J.-C.; Knight, B.; Wudl, F. *J. Am. Chem. Soc.* **1996**, *118*, 13081–13082. (b) Hutchison, K.; Srdanov, G.; Menon, R.; Gabriel, J.-C.; Knight, B.; Wudl, F. *Synth. Met.* **1997**, *86*, 2147–2148.

(35) Morton, J. R.; Preston, K. F. *J. Magn. Reson.* **1978**, *30*, 577–582.

(36) McConnell, H. M. *J. Chem. Phys.* **1958**, *28*, 1188–1192.

(37) (a) Singel, D. J.; van der Poel, W. A. J. A.; Schmidt, J.; van der Waals, J. H.; de Beer, R. *J. Chem. Phys.* **1984**, *81*, 5453–5461. (b) Stoll, S.; Jahromy, Y. N.; Woodward, J. J.; Ozarowski, A.; Marletta, M. A.; Britt, R. D. *J. Am. Chem. Soc.* **2010**, *132*, 11812–11823.

(38) Luzon, J.; Campo, J.; Palacio, F.; McIntyre, G. J.; Rawson, J. M.; Less, R. J.; Pask, C. M.; Alberola, A.; Farley, R. D.; Murphy, D. M.; Goeta, A. E. *Phys. Rev. B* **2010**, *81*, 144429−1–144429−12.

(39) (a) Baker, G. A., Jr.; Rushbrooke, G. S.; Gilbert, H. E. *Phys. Rev. A* **1964**, *135*, 1272–1277. (b) Swank, D. D.; Landee, C. P.; Willet, R. D. *Phys. Rev. B* **1979**, *20*, 2154–2162.

(40) (a) Ising, E. *Z. Phys.* **1925**, *31*, 253–258. (b) Kahn, O. *Molecular Magnetism*; VCH Publishers, Inc.: New York, 1993.

(41) Dietrich, M.; Heinze, J. *J. Am. Chem. Soc.* **1990**, *112*, 5142–5145.

(42) Public EPR Software Tools: *Winsim Spectral Simulation for MS-Windows 9x, NT v0.98*; O'Brien, D. A.; Duling, D. R.; Fann, Y. C. NIEHS, National Institute of Health, Bethesda, MD.

(43) *CrysAlis CCD and CrysAlis RED, version p171.33.34d*; Oxford Diffraction Ltd: Abingdon, Oxford, England, 2009.

(44) (a) Altomare, A.; Cascarano, G.; Giacovazzo, C.; Guagliardi, A.; Burla, M. C.; Polidori, G.; Camalli, M. SIR92. *J. Appl. Crystallogr.* **1994**, *27*, 435–436. (b) Sheldrick, G. M. *SHELXL97*; University of Göttingen: Germany.

(45) (a) Brandenburg, K. *DIAMOND. Version 3.1d*; Crystal Impact GbR: Bonn, Germany, 2006. (b) Macrae, C. F.; Edgington, P. R.; McCabe, P.; Pidcock, E.; Shields, G. P.; Taylor, R.; Towler, M.; van de Streek, J. MERCURY: Visualization and analysis of crystal structures. *J. Appl. Crystallogr.* **2006**, *39*, 453–457.

(46) Frisch, M. J.; Trucks, G. W.; Schlegel, H. B.; Scuseria, G. E.; Robb, M. A.; Cheeseman, J. R.; Montgomery, J. A., Jr.; Vreven, T.; Kudin, K. N.; Burant, J. C.; Millam, J. M.; Iyengar, S. S.; Tomasi, J.; Barone, V.; Mennucci, B.; Cossi, M.; Scalmani, G.; Rega, N.; Petersson, G. A.; Nakatsuji, H.; Hada, M.; Ehara, M.; Toyota, K.; Fukuda, R.; Hasegawa, J.; Ishida, M.; Nakajima, T.; Honda, Y.; Kitao, O.; Nakai, H.; Klene, M.; Li, X.; Knox, J. E.; Hratchian, H. P.; Cross, J. B.; Bakken, V.; Adamo, C.; Jaramillo, J.; Gomperts, R.; Stratmann, R. E.; Yazyev, O.; Austin, A. J.; Cammi, R.; Pomelli, C.; Ochterski, J. W.; Ayala, P. Y.; Morokuma, K.; Voth, G. A.; Salvador, P.; Dannenberg, J. J.; Zakrzewski, V. G.; Dapprich, S.; Daniels, A. D.; Strain, M. C.; Farkas, O.; Malick, D. K.; Rabuck, A. D.; Raghavachari, K.; Foresman, J. B.; Ortiz, J. V.; Cui, Q.; Baboul, A. G.; Clifford, S.; Cioslowski, J.; Stefanov, B. B.; Liu, G.; Liashenko, A.; Piskorz, P.; Komaromi, I.; Martin, R. L.; Fox, D. J.; Keith, T.; Al-Laham, M. A.; Peng, C. Y.; Nanayakkara, A.; Challacombe, M.; Gill, P. M. W.; Johnson, B.; Chen, W.; Wong, M. W.; Gonzalez, C.; Pople, J. A. *Gaussian 03, revision C.02*; Gaussian, Inc.: Wallingford, CT, 2004.